

# Mass determination of astrometric binaries with Hipparcos

## II. Selection of candidates and results

C. Martin and F. Mignard

Observatoire de la Côte d'Azur, CERGA, UMR CNRS 6527, av. N. Copernic, F-06130 Grasse, France

Received 23 July 1997 / Accepted 20 August 1997

**Abstract.** In a previous paper (Martin et al., 1997) we have shown that for double stars with orbital periods smaller than about 25 years, it was possible to determine from the Hipparcos data, the mass ratio  $B$  of the components or the difference between the mass and intensity ratios,  $\beta - B$ , provided the orbital elements of the relative orbit are available. From an extensive literature search we have selected 145 potential systems, of which 46 yielded eventually a satisfactory solution. For eight systems with the largest separations, the peculiarities of the natural direction associated to the Hipparcos observations, the 'hippacentre', have been fully exploited to derive the mass ratio of the components without any additional assumption. For the remaining 38, the derivation of the mass ratio was possible only by taking the magnitude difference between the two components from other sources. The parallax determined simultaneously, is then used to produce the individual masses of the components. The astrophysical relevance of the results is discussed and when possible (17 systems) the masses are compared to ground-based values.

**Key words:** stars: distances – binaries: visual – astrometry – stars: fundamental parameters

---

### 1. Introduction

The data processing of the Hipparcos observations was conducted by keeping the number of hypotheses regarding the structure of the light sources to minimum. In particular the signal recorded behind the grid was compressed in such a way that no information linked to a possible multiplicity was lost during this process, allowing at a latter stage to recover the individual sources and their relative position and brightness. A similar care was applied to the astrometric model used to describe the varying position of the sources on the sky, keeping all the way through the analysis the possibility to decide whether the detected motion was linear or accelerated, or even more complex in order to select the model accordingly.

---

*Send offprint requests to:* F. Mignard (mignard@obs-azur.fr)

When a Hipparcos target was a single object, the standard astrometric model in the data reduction assumed a uniform rectilinear motion in space relative to the barycentre of the solar system. In this case only five parameters were necessary to describe the full astrometric information embedded in the Hipparcos measurements: the two angular coordinates to specify the coordinate direction at the Catalogue epoch ( $T_0 = \text{J1991.25}$ ), the two components of the proper motion used to propagate this position at any other past or future epochs and the parallax, which, besides its obvious astrophysical interest, allows to determine the proper direction from the Earth.

In the case of a non single object, known before the mission or recognized by Hipparcos, the situation was more complex and additional parameters were needed to model properly the observations, the number of which was variable with the type of multiple system. The treatment was much influenced by the separation and the period of the orbital motion, and corresponds more or less to the usual distinction made for the ground-based observations, between the visual and the astrometric binaries.

For double stars with an orbital period much longer than the duration of the Hipparcos mission, the data processing was adapted to cope with this difficulty and eventually this led to a good decoupling between the relative and absolute astrometry for more than 13 000 binary systems included in the Catalogue. The various principles applied to the recognition of these systems and the properties of the relative and absolute astrometric solution have been presented in detail in the literature (Mignard et al, 1992, Mignard et al, 1995) and will not be repeated here. The definitive and most detailed information is now available directly in the Hipparcos documentation (ESA, 1997).

In this work, we are more concerned with the close pairs with an orbital period less than 10 years which could exhibit a significant non-linear motion of their photocentre over the observation timespan. The amplitude of this motion is related to the size of the relative orbit of the two components and to the difference between the mass and intensity ratio.

For very close binaries with a maximum separation less than few mas, the satellite could not show any photocentric displacement beyond the linear proper motion of the barycentre and the entries were processed in the same way as the single stars. The

most interesting cases, as far as the masses are concerned, are to be found in the orbital pairs which fulfilled the following two criteria :

1. a significant apparent separation,  $\rho > 100$  mas,
2. an orbital period comparable or a few times larger than the mission lifetime.

Obviously these two constraints imply that the interesting systems are located not very far from the solar system, a circumstance favorable to obtain the parallax with a good relative precision and consequently to determine the total mass of the system, but at the same time a very demanding constraint which considerably narrows the number of good candidates.

In these cases the curved or wavy displacement of the photocentre was significant and could be separated from the proper motion, provided provision for such a motion was made in the astrometric modeling. Although it was practically impossible to determine the full set of orbital elements only from the Hipparcos observations, it is well known that the photocentric orbit and the relative orbit are similar in shape, differing by a scale factor which depends only on the mass of the components and on the magnitude difference. Therefore, including this scale factor as an additional unknown to the standard astrometric model, permits to derive the masses of the components alongside the positions, parallax and proper motion. Martin et al., 1997, have shown how to extend this basic property to the one dimensional Hipparcos observations and that, in some cases, both the mass ratio and the intensity ratio could be derived from the absolute motion of the Hippacentre, when the latter could be decoupled from that of the photocentre.

The first paper (Martin et al., 1997) dealt primarily with the methodology. The capabilities and limitations of the method were primarily assessed from a monte-Carlo simulation and the paper ended with a short list of likely good systems worth testing. In this second paper we apply the method to more than 40 real systems of the Hipparcos program, found to have the appropriate characteristics. The first section sums up the sources of the orbital data and closes with the selection of the  $\approx 140$  systems for which a solution should be attempted. The processing is presented in the second section and the astrometric results are shown and discussed in the following section. The masses are derived in the fourth section together with the discussion of their reliability and the comparison to published results.

## 2. The selection of systems and orbits

### 2.1. The sources of data

According to the results of the simulation presented in Martin et al., 1997, the search of astrometric binaries likely candidates for a mass determination from the Hipparcos observations, must be restricted to pairs with orbital periods smaller than or equal to 30 years. Another selection based on the separation will be considered later. Four main sources of orbits were used to identify the potential systems :

**Table 1.** HIP numbers of the 145 preselected systems

HIP	HIP	HIP	HIP	HIP	HIP	HIP
171	16467	29850	49658	76852	91394	105431
2237	16628	30920	49929	78401	92122	107162
2533	19508	31509	51147	78662	93506	107354
2762	19719	31978	51986	80346	93574	107522
2941	19758	32800	54204	80816	94144	107788
4463	20661	33451	64241	81470	94349	107849
5300	20686	38052	64375	82817	94643	108195
6564	20894	38382	64838	83838	94739	108431
7580	21281	39261	65069	84140	94847	111528
7918	21880	41261	66008	85141	95477	111805
10535	22196	41426	66640	85846	96683	111965
11452	22550	41489	69514	86032	98001	111974
12390	23170	42075	70576	86221	98416	112158
12421	23395	43671	70973	87204	100266	112746
12552	23835	44248	71094	87655	101769	113323
12623	24608	45170	72217	87895	101958	113445
12717	26926	45571	72479	87991	103055	113996
13531	28614	45999	74000	88498	103655	116849
14328	28734	46706	74392	88637	104771	117666
14576	29234	47479	75695	88932	104858	
15868	29746	47758	76041	89937	104978	

1. A file of orbits available at the Observatory of Côte d'Azur from P. Morel and P. Coureau (identified by 'OCA' in Tables 4-5). It is indeed a compilation of orbits coming from several sources, and particularly from the Catalogue of Worley. It includes 905 orbits of 800 systems and contains additional information like the magnitude at 550 nm. It happens that several orbits may be proposed for the several pairs or for hierarchical systems containing more than one pair, which explains that the number of orbits is larger than the number of systems.
2. The file of orbits from the Royal Observatory of Belgium kindly provided by J. Dommange, containing 864 orbits of 838 systems ('ORB' in Tables 4-5).
3. The fourth catalog of orbits of visual binary stars (Worley & Heintz, 1983), including 928 orbits for 847 systems (a triple star being identified as two systems).
4. Finally, searches in the published literature were necessary to update the information contained in the previous files and provided several new orbits recently computed.

The above sources are in practice largely redundant. The intersection of these four sources and that of the Hipparcos observing program combined with the limitation in period, yields at the end a set of 302 orbits for 191 different entries of the Hipparcos Catalogue. This constitutes the basic data set to be investigated.

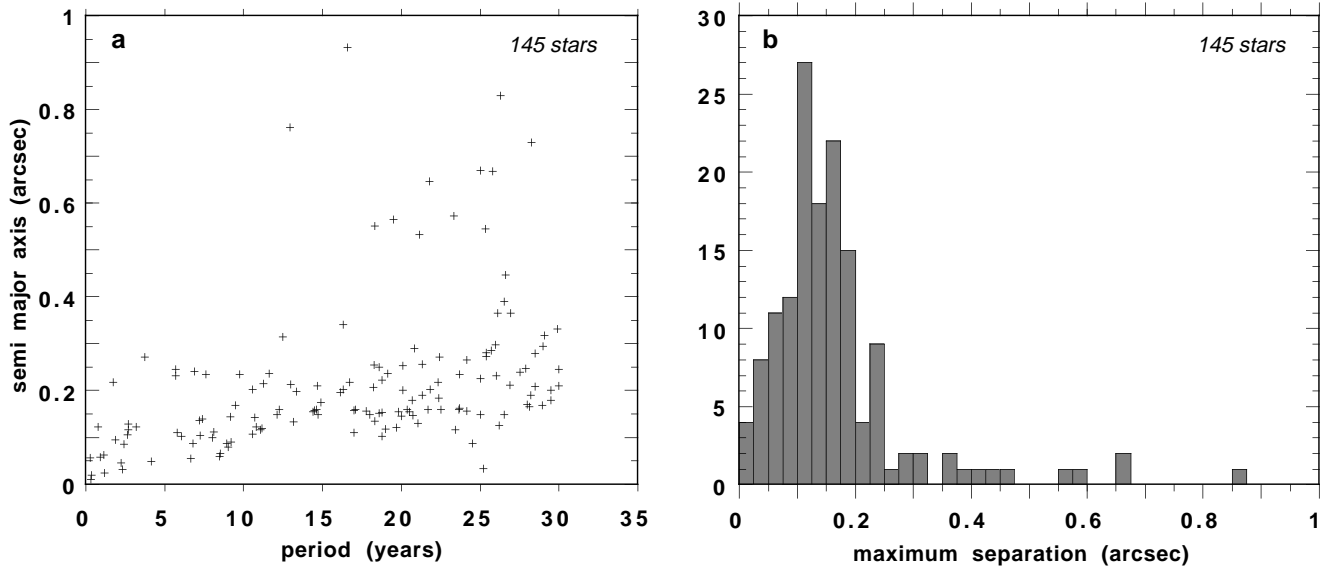


**Fig. 1a and b.** Statistical description of the file of 145 orbital pairs with periods smaller than 30 years. The most recent orbit has been chosen for each object. In **b** the abscissa is the largest apparent separation over the orbital period.

## 2.2. Elimination of objects

Among these 191 objects, there are several systems which cannot be processed by the method of Paper I, because of the parasitic effect of a third component in the vicinity ( $< 25''$ ) of the central pair. This led to the rejection of 16 systems from the initial set. In addition, two more systems were eliminated as they were finally not successfully observed by the satellite (HIP 21088 and HIP 116191). After this step, we were left with 277 orbits for 173 objects.

There were in this sample 28 astrometric pairs for which the published orbits referred to the absolute motion of the photocentre on the sky, instead of the relative motion of the two components. In this case, nothing more could be done with the Hipparcos data and these stars had to be removed from the sample. Eventually, the useful sample numbers 242 orbits associated to 145 objects listed in 1 by their HIP identifier.

## 2.3. Description of the subset of binaries

### 2.3.1. Statistical description

The first description proposed here aims to recognize the pairs for which the independent determination of the mass and intensity ratios seems possible, from those for which the values of the period and the separation will not allow this distinction. Fig. 1a reveals a non negligible population of interesting pairs with semi-major axes larger than  $0''.25$ , but also with periods generally larger than 15 years. It shows also the difficulty, expected indeed, to find binaries with both large separations and small periods. Fig. 1b shows the distribution of the largest separation on the sky reached by every pair during a complete revolution (as long as the Hipparcos observations are concerned, this quantity is more representative than the semi-major axis).

### 2.3.2. An adapted characterization

As the sample of objects considered is not too large (compared to the whole set of about 12000 binaries for which an astrometric solution is published in the final Hipparcos Catalogue), it has been possible to define an 'identity card' of each selected star, allowing to illustrate the potential of Hipparcos in each case. In the following diagrams, each 'card' appears as a segment and four numbers, with the following meanings:

- The number in abscissae of each segment is the Hipparcos identifier of the star (HIP number).
- The ordinates at the top and bottom of the segment represent the maximum and the minimum apparent separations reached by the double star during an orbital period, computed from the orbital elements.
- An open box on each segment shows the range of apparent separations covered by the Hipparcos observations during the 3 years of the mission.
- The number of epochs of observations stands on the right of each box. An epoch corresponds to a combination of a few consecutive observations carried out within one or two days, while the interval between two epochs is typically of six weeks; the different epochs are generally well distributed in time over the mission duration.
- The approximate global Hipparcos magnitude of the object and the orbital period in years (from the most recent orbit determination) are indicated at the top of each segment.

This information is displayed in Fig. 2. Independently, on each diagram three horizontal lines have been drawn and represent the theoretical thresholds in apparent separation beyond which it becomes possible to distinguish the photocentre and the Hipparcos centre of the star, for a system of 2 mag (bottom line), 10 mag (middle line) and 12 mag (top line). In connection with the re-

**Table 2.** The set of astrometric binaries for which a ground-based orbit has been used to reprocess the Hipparcos observations for determining the mass of the components. The columns give the Hipparcos, ADS and HD identifiers, the usual name, the semi-major axis of the relative orbit in arcsec and the orbital period in years.

HIP	ADS	HD	Name*	$a''$	$P$ (yr)	HIP	ADS	HD	Name*	$a''$	$P$ (yr)
171	17175	224930	85 Peg	0.830	26.27	2237	—	2475	B 1909	0.214	11.25
2762	490	3196	13 Cet	0.240	6.89	7580	—	10009	Kui 7	0.318	29.05
12390	—	16620	$\epsilon$ Cet	0.105	2.65	14328	2324	18925	$\gamma$ Per	0.159	14.65
14576	2362	19356	Algol	0.095	1.86	19508	3041	26441	A 2801	0.145	20.00
19719	3064	26690	46 Tau	0.135	7.18	22196	—	30090	—	0.087	6.81
23170	3552	31337	Hu 1090	0.232	26.00	24608	3841	34029	Capella	0.056	0.28
29850	4890	43525	75 Ori	0.090	9.20	31509	—	47230	Fin 19	0.295	29.00
38052	6354	62522	Hu 1247	0.200	18.80	39261	—	65339	53 Cam	0.055	6.64
43671	—	76360	Fin 316	0.104	7.24	44248	—	76943	10 Uma	0.647	21.78
45170	—	79096	81 Cnc	0.116	2.70	54204	—	96202	$\chi$ 01 Hya	0.140	7.40
64838	—	115488	—	0.080	9.05	75695	—	137909	$\beta$ CrB	0.203	10.55
78401	—	143275	$\delta$ Sco	0.107	10.58	80346	—	—	GL 623	0.271	3.73
82817	—	152751	Kui 75	0.218	1.71	83838	10360	155103	c Her	0.112	8.13
84140	—	155876	Kui 79	0.762	12.95	85141	—	157498	Rst 3972	0.148	14.73
86032	—	159561	Rasalhague	0.483	8.67	87204	—	162338	—	0.179	20.70
87655	—	163151	—	0.087	8.92	87895	—	163840	—	0.085	2.41
89937	—	170153	$\chi$ Dra	0.122	0.77	91394	11520	172088	A 88	0.196	12.18
93574	—	175986	Fin 357	0.155	14.38	94349	—	—	GL 748	0.130	2.30
94739	—	179930	Rst 4036	0.234	7.61	96683	—	185734	$\phi$ Cyg	0.024	1.19
98416	—	189340	GL 773.3	0.234	9.74	104771	14761	202128	—	0.231	5.70
104858	14773	202275	$\delta$ Equ	0.245	5.71	105431	14893	203345	A 617	0.102	6.05
107354	15281	206901	$\kappa$ Peg	0.255	11.56	108431	—	208450	$\delta$ Ind	0.127	6.09
112158	16211	215182	$\eta$ Peg	0.045	2.24	116849	—	222516	Mlr 4	0.147	20.75

\* When available, the more common name of the star, or the Gliese catalog number.

sults of the simulation of Paper I, the previous representation allows to estimate quickly what can be expected from the processing of each star, assuming that the orbit is perfectly known. However only about 25% of the published orbits are considered as 'very good' or 'definitive' according to the criteria of the Worley's catalog; this is probably the main reason why significant results could not be obtained for all of the stars considered here.

### 3. Important points of the data processing

#### 3.1. General management

The practical implementation of the processing is briefly described in Paper I, Sect. 4.2. There is a double iterative process: the first one consists in improving the reference values ( $\beta_r$ ,  $B_r$ ) at the step  $i$  by injecting the solutions obtained at step  $(i-1)$ ; the second one corresponds to the iterative filtering of the largest residuals found in this step. The data of the 145 selected objects have first been processed by an *all purpose* algorithm, quite similar to the one used for the simulation. However the poor overall quality of the results has shown that a specific processing adapted for each star was preferable. One of the most

crucial points to ensure the convergence of the processing was the choice of the threshold to filter out the residuals and this had to be fine-tuned on a case by case basis alongside the weighing of the observations.

#### 3.2. The reference values of $\beta$ and $B$

As it was mentioned in Paper I, Sect. 4.2, the equations relating the Hipparcos observations on the circle to the astrometric and physical parameters are all non-linear. Thus, it is useful to start the processing with input values of  $\beta$  and  $B$  relatively good. It turns out that for all the cases presented in this paper, the magnitude difference is fairly well known and this was sufficient to compute an input  $\beta$ . On the other hand, for more than half of the systems, no reliable input value of the mass ratio  $B$  has been found (see Table 9). In this case the mass luminosity relation for dwarf stars has been used to yield an approximate first guess of  $B$  via the expression,

$$\Delta m \approx 7 \log \left( \frac{M_1}{M_2} \right) \Leftrightarrow B \approx (1 + 10^{+0.14\Delta m})^{-1} \quad (1)$$

where  $M_1$  and  $M_2$  are the masses of the components.

**Table 3.** Same set as in Table 3, showing the Hipparcos results from the standard processing. The labels C, O, G, X refer to the sections of the Double and Multiple Systems Annex in which the solution has been placed. A blank in this column indicates that a single star solution has been adopted.

HIP	$\pi$ (mas)	$\sigma_\pi$	$Hp$		HIP	$\pi$ (mas)	$\sigma_\pi$	$Hp$		HIP	$\pi$ (mas)	$\sigma_\pi$	$Hp$	
171	80.6	3.0	5.874	X	2237	31.0	0.9	6.558	C	2762	47.5	1.1	5.321	C
7580	26.1	0.8	6.355	G	12390	37.0	1.8	4.926	C	14328	12.7	0.7	3.059	O
14576	35.1	0.9	2.097	O	19508	15.9	1.0	7.496		19719	27.0	0.9	5.374	O
22196	14.1	0.9	6.672		23170	12.1	0.9	8.489	C	24608	77.3	0.9	0.239	O
29850	12.9	0.8	5.433		31509	24.8	0.6	6.467	C	38052	26.6	0.8	7.141	C
39261	10.2	0.8	6.076	G	43671	12.5	0.5	5.384	O	44248	60.9	1.3	4.059	C
45170	48.8	0.9	6.626		54204	23.0	0.7	5.009	O	64838	13.4	0.8	6.433	
75695	28.6	0.7	3.737	O	80346	124.3	1.2	10.313	O	82817	174.2	3.9	9.014	C
83838	18.5	0.6	5.484	O	84140	158.2	3.3	9.375	C	85141	15.5	1.2	7.967	G
86032	69.8	0.9	2.126	G	87204	18.8	0.6	7.287	C	87655	14.7	0.8	6.343	G
87895	35.0	0.6	6.454	O	89937	124.1	0.5	3.667	O	91394	4.8	0.9	8.390	
93574	17.6	0.8	5.997	C	94349	98.6	2.7	11.103	O	94739	63.4	2.2	9.446	C
96683	13.0	0.6	4.839	O	98416	40.8	1.4	5.997	C	104771	11.2	0.8	6.3370	C
104858	54.1	0.9	4.593	C	105431	21.5	0.8	6.832	O	107354	28.3	0.9	4.235	C
108431	17.6	0.8	4.478	C	112158	15.2	0.8	3.090	O	116849	14.4	0.8	7.079	C

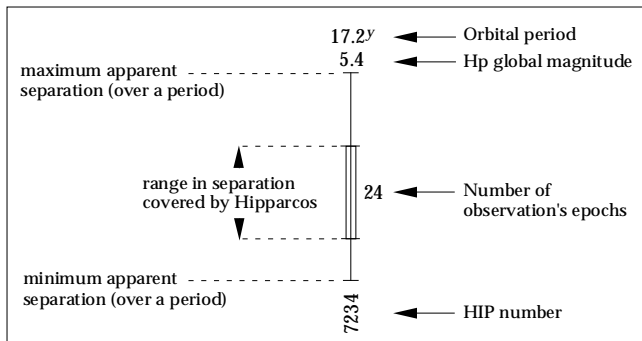


**Fig. 2.** Description of the sample of short period binaries, as found in the diagrams of Fig. 3. If the orbit is perfectly known, the ability of Hipparcos to obtain the mass ratio directly is as important as the global magnitude and the period are small, as the number of observation's epochs is large, as the range in separation covered by Hipparcos is large compared to the total possible range on the sky (size of the segment), and as the separations observed are large.

### 3.3. The choice of an orbit

For many of the systems, there are more than one set of orbital elements proposed in the literature. We have tested systematically all the possible orbits for each object and then selected a particular set of orbital elements. The selection criteria were based on the quality of the fit (Unit Weight Variance), the number of required iterations and the stability of the solutions to a small perturbation of the input values and of the orbital elements. For most of the cases, the selected orbit (see Tables 4-5) happens to be the most recent one. It must also be noted that the

elements derived from the speckle interferometry were particularly satisfactory, regarding their adequation to the Hipparcos data.

## 4. Raw results

### 4.1. Presentation

Significant results have been obtained for 46 systems among the 145 tested. This sample has been divided into 2 categories, called Type I and Type II solutions, defined as,

1. **Type I** : the separation is large enough to allow a separate determination of the intensity and mass ratios  $\beta$  and  $B$  with an absolute accuracy better than 0.07. The number of unknowns in the model is seven (The five usual astrometric parameters  $l$ ,  $b$ ,  $\pi$ ,  $\mu_l$  and  $\mu_b$  related to the centre of mass and the two ratios  $\beta$  and  $B$ ).
2. **Type II** : binaries with smaller separations; the motion observed is the photocentric orbit combined to the rectilinear motion of the centre of mass. We only determine the scale factor  $\beta - B$  and the astrometric parameters previously defined (six unknowns).

The solutions are presented in Tables 4 and 5 for 8 Type I and 38 Type II binaries. The full description of the columns is given below Table 4.

When several orbits are proposed for a system, quite often two of them differ only by a difference of  $\pm 180$  degrees of one of the angles  $\omega$  (periastron argument) or  $\Omega$  (position angle of the ascending node). This is equivalent to invert the choice of the primary between the two components. In this case we

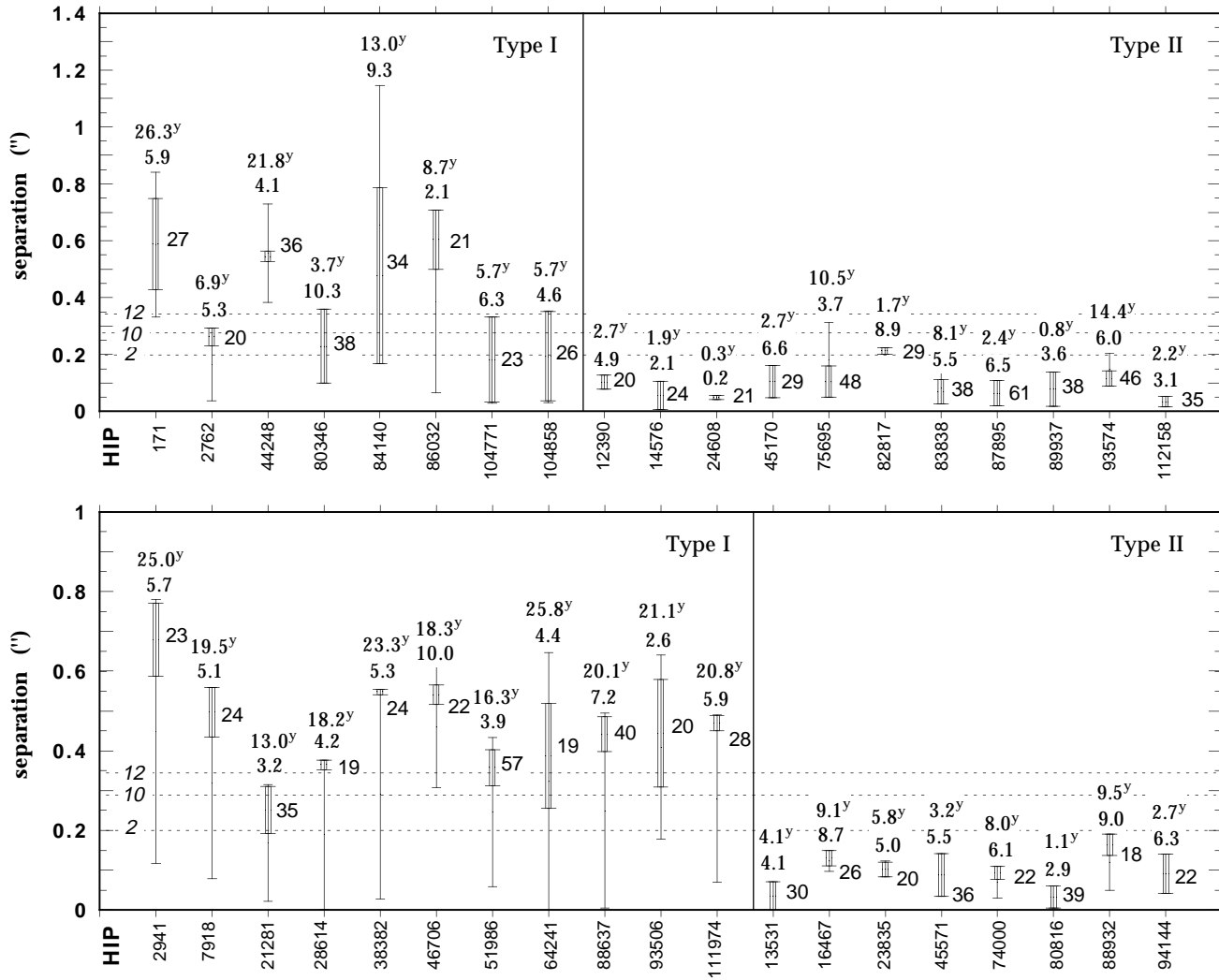


**Fig. 3.** Individual description of some interesting binary systems as sketched out in Fig. 2. The top diagram contains stars for which a solution has been found, divided into 'Type I' and 'Type II' solutions. On the bottom diagram are represented some potentially interesting stars (the processing can be successful for these objects if the knowledge of the orbit is improved). The three horizontal lines, labelled by the global magnitude  $H_p$ , are the theoretical thresholds in separation beyond which photocentre and hippacentre are no longer alike. Caution: the vertical scales are different in the two diagrams.

only kept one representative orbit and systematically tested the alternate possibility. Formally, this transformation implies that one gets  $(1 - \beta)$  and  $(1 - B)$  instead of  $\beta$  and  $B$ . Thus, when the two ratios are combined to form the scale of the photocentric orbit, we get  $-(\beta - B)$  instead of  $(\beta - B)$ . In several instances it was difficult to make a choice between the two solutions, as their quality were almost identical, and then we decide to retain the solution based on the published (not rotated) orbit. When the system was sufficiently well known to constrain the sign of  $\beta - B$ , the exchange of the components, if necessary, is indicated in the Tables 4-5 by the minus sign '-' in the third column. In particular this is the case for Algol AB-C: the sign '-' informs that one of the two angles  $\Omega$  or  $\omega$  must be increased by 180 degrees to make the orbit consistent with the Hipparcos observations.

#### 4.2. Discussion

As mentioned above, the quantity  $(\beta - B)$  represents the scale factor between the photocentric orbit and the relative orbit. Practically, if the semi-major axis  $a$  found in the literature is wrong by a factor  $\alpha$ , we get, instead of  $\beta - B$ , a quantity  $(\beta - B)/\alpha$ , so that the product  $a(\beta - B)$  is constant. This phenomenon affects all the Type II solutions, where the hippacentre and the photocentre are alike. A quantification of this effect can be achieved from the propagation of the standard error of the semi-major axis,  $\sigma_a$  to  $(\beta - B)$ :

$$\sigma_{\beta-B}^2 = \sigma_K^2 + \left(\frac{K}{a}\right)^2 \sigma_a^2 \quad (2)$$

where  $K$  and  $\sigma_K$  are respectively the scale factor (i.e. the biased estimate of  $\beta - B$ ) and its standard error, both given by the

**Table 4.** Astrometric binaries processing. Raw results for eight systems with a solution of first type.

HIP	orbit ref.	orient.	$N_i$	$N_p$	$\beta - B$	$\sigma$	$(\beta - B)_r$	$\sigma$	$B$	$\sigma$	$B_r$	$\sigma$
171	Hall49	+	3	7	-0.481	0.036	-0.403	—	0.528	0.034	0.453	—
2762	Hartkopf89	+	7	7	-0.166	0.051	—	—	0.400	0.059	—	—
44248	Hartkopf96	+	4	7	-0.269	0.025	-0.294	0.065	0.409	0.023	0.426	0.061
80346	Henry93	+	2	7	-0.177	0.012	-0.177	0.021	0.204	0.027	0.183	0.02
84140	Hartkopf96	+	4	7	-0.046	0.018	-0.087	0.045	0.443	0.05	0.496	0.01
86032	Augensen92*	—	3	7	-0.139	0.017	-0.132	0.031	0.147	0.016	0.17	0.03
104771	Hartkopf96	+	5	7	0.021	0.021	—	—	0.457	0.028	—	—
104858	ORB	—	8	7	0.039	0.021	-0.064	0.046	0.457	0.032	0.497	0.008

\* The semi major axis of the relative orbit is taken in Kamper 89.

orbit ref. : identifier of the orbit (see references).

orient. : The orientation is that of the published orbit (+) or has been reversed from the examination of the residuals (—).

$N_i, N_p$  : Number of iterations and number of unknowns in the model.

$\beta - B, B$  : solutions of the reduction followed by the corresponding standard errors.

$(\beta - B)_r, B_r$  : reference values used to start the algorithm (see Table 9).

processing, and assimilated to  $\beta - B$  and its standard deviation in the Tables 4 and 5.

A quantification of this effect has been made by taking the set of the standard deviations of the semi-major axes of the 46 orbits, and calculating the ratio  $r = (\sigma_{\beta-B} - \sigma_K)/\sigma_K$  in each case, with the previous expression. The information on  $\sigma_a$  has been found for only half the systems, giving a median value of the  $r$  distribution of only 0.02%. The ratio exceeds 2% for two objects: HIP 87895 ( $r \approx 21\%$ ) and HIP 89937 ( $r \approx 9\%$ ). However, this study may be biased: the orbits for which the standard errors are published are probably the best ones. Moreover, most of the orbits among the 23 were computed very recently from speckle interferometry, with relative errors on the semi-major axis ranging from 0.07% to 6%.

## 5. Mass determination

### 5.1. Strategy

The first step is the determination of the total mass  $M$  of the system with the Kepler's third law. The estimate of the parallax  $\pi$  is one of the six or seven unknowns solved in the processing (Martin et al., 1997), while the period  $P$  and the semi-major axis  $a$  of the relative orbit are taken from the literature. The references for the orbital elements are given in Tables 4-5. The combination of the uncertainty of the orbital period and that of the parallax is easily propagated in the standard deviation of the total mass as,

$$\sigma_M = M \sqrt{9 \left(\frac{\sigma_a}{a}\right)^2 + 9 \left(\frac{\sigma_\pi}{\pi}\right)^2 + 4 \left(\frac{\sigma_P}{P}\right)^2} \quad (3)$$

Unfortunately, the errors of the orbital elements are not systematically published. Instead of estimating rather arbitrarily the missing quantities, we have calculated for each mass an incomplete error, and have indicated the nature of the missing element(s) in Tables 7-8 by the flag noted  $N$ . When  $N = 3$ ,

the three error estimates  $\sigma_\pi, \sigma_P$  and  $\sigma_a$  were known. On the other hand,  $N = 2$  or  $N = 1$  mean that only  $\sigma_P$  or both  $\sigma_P$  and  $\sigma_a$  were unknown. Whereas the knowledge of  $\sigma_P$  is not essential (the weight of this term is 2.3 times smaller than the two others, and  $P$  is generally the best known parameter for such short-period binaries), this is no longer true for the semi-major axis. The cases with  $N = 1$  correspond to underestimating the variance of the total mass, and thus must be considered with caution.

In a second step we combine the mass ratio  $B = M_2/M$  of the components with the total mass in order to obtain the individual masses:

$$M_1 = M(1 - B) \quad , \quad M_2 = M.B \quad (4)$$

Two situations must be distinguished:

1. The mass ratio  $B$  is the solution of the processing (Type I stars), so that Eq. 4 is directly implemented and yields the two masses (100% Hipparcos results). This method is flagged 'A' in Table 7.
2. The only available ratio is the difference  $\beta - B$  (Type II stars). In that case, we use a ground-based estimate of the magnitude difference  $\Delta m$  in a  $V$  band to calculate  $\beta$ , and then  $B$ . This is flagged method 'B' in Table 7. The results obtained in this way are of course less accurate than the previous ones, because of the heterogeneity of the quantities involved. To improve the quality, the magnitude differences have been expressed, when possible, in the Hipparcos photometric system (see next section).

For solutions of the second type, the variance of the mass ratio  $B$  is computed from a combination of the variances of  $(\beta - B)$  and  $\Delta m$ :

$$\sigma_B^2 \approx \sigma_{\beta-B}^2 + 0.848 \beta^2 (\beta - B)^2 \sigma_{\Delta m}^2 \quad (5)$$

**Table 5.** Astrometric binaries processing. Raw results for 38 stars with solutions of second type. For two stars (HIP 31509 and HIP 107354), results from method B ( $N_p = 7$ ) are also presented, as these stars are 'quasi' Type I objects.

HIP	orbit ref.	orient.	$N_i$	$N_p$	$\beta - B$	$\sigma$	$(\beta - B)_r$	$\sigma$	$B$	$\sigma$
2237	V.d.Bos56	+	5	6	0.019	0.017	—	—	—	—
7580	Hartkopf96	+	4	6	-0.172	0.034	—	—	—	—
12390	Hartkopf89	+	3	6	0.142	0.009	0.084	—	—	—
14328	McAlister82	—	2	6	-0.122	0.020	-0.152	—	—	—
14576	Pan93	—	2	6	-0.202	0.005	-0.210	0.020	—	—
19508	Muller54	+	2	6	0.034	0.024	—	—	—	—
19719	Hartkopf96	+	2	6	-0.134	0.020	—	—	—	—
22196	Baize93	+	2	6	0.014	0.017	—	—	—	—
23170	OCA	+	2	6	-0.015	0.031	—	—	—	—
24608	Hummel94	+	2	6	-0.037	0.014	-0.022	0.013	—	—
29850	Hartkopf96	+	3	6	-0.012	0.044	—	—	—	—
31509	Finsen77	+	4	7	-0.140	0.062	—	—	0.484	0.120
31509	Finsen77	+	3	6	-0.166	0.048	—	—	—	—
38052	Hartkopf96	+	3	6	0.098	0.063	—	—	—	—
39261	Hartkopf96	+	4	6	-0.358	0.084	—	—	—	—
43671	Finsen73	+	5	6	0.257	0.043	—	—	—	—
45170	Mason96	+	3	6	0.030	0.007	-0.043	—	—	—
54204	V.d.Bos57	+	2	6	0.029	0.018	—	—	—	—
64838	Hartkopf96	+	3	6	0.038	0.056	—	—	—	—
75695	Kamper90	+	2	6	-0.273	0.009	-0.234	0.044	—	—
78401	Hartkopf96	+	4	6	-0.038	0.043	—	—	—	—
82817	Voute46	+	4	6	-0.132	0.008	—	—	—	—
83838	Hartkopf89	+	3	6	0.054	0.013	—	—	—	—
85141	Hartkopf96	+	4	6	-0.163	0.059	—	—	—	—
87204	Hartkopf96	+	4	6	-0.074	0.062	—	—	—	—
87655	Hartkopf96	+	3	6	0.214	0.042	—	—	—	—
87895	McAlister95	+	2	6	-0.317	0.011	-0.329	0.061	—	—
89937	Tomkin87	—	3	6	-0.319	0.006	-0.283	0.044	—	—
91394	V.d.Bos53	+	8	6	0.138	0.062	—	—	—	—
93574	Heintz84	+	3	6	-0.052	0.013	—	—	—	—
94349	Harrington77	+	3	6	-0.246	0.031	-0.229	—	—	—
94739	Heintz84	+	9	6	0.119	0.066	—	—	—	—
96683	Armstrong92	+	3	6	-0.076	0.023	-0.059	0.046	—	—
98416	Hartkopf96	—	4	6	0.280	0.10	—	—	—	—
105431	West76	—	3	6	0.119	0.017	0.094	—	—	—
107354	Hartkopf89	+	3	7	-0.152	0.015	—	—	0.556	0.069
107354	Hartkopf89	+	3	6	-0.148	0.015	—	—	—	—
108431	Churms65	+	4	6	-0.136	0.067	—	—	—	—
112158	Hummel92	+	3	6	-0.287	0.013	—	—	—	—
116849	Hartkopf96	+	5	6	-0.107	0.072	—	—	—	—

In any case, the errors on the individual masses are given by the classical expressions:

$$\sigma_{M_1} = M_1 \sqrt{\left(\frac{\sigma_M}{M}\right)^2 + \left(\frac{\sigma_B}{1-B}\right)^2} \quad (6)$$

$$\sigma_{M_2} = M_2 \sqrt{\left(\frac{\sigma_M}{M}\right)^2 + \left(\frac{\sigma_B}{B}\right)^2} \quad (7)$$

### 5.2. The photometric transformation

To transform the ground-based estimates of  $\Delta m$  into the Hipparcos system, the knowledge of the spectral types of each component is required. They have been found for only 18 systems over the 38 binaries for which it was really needed, mainly by the use of the SIMBAD database. The result of this survey is summarised in Table 6, with the corresponding Johnson's  $V-I$  colour indices.

The four steps of the photometric conversion are the following:



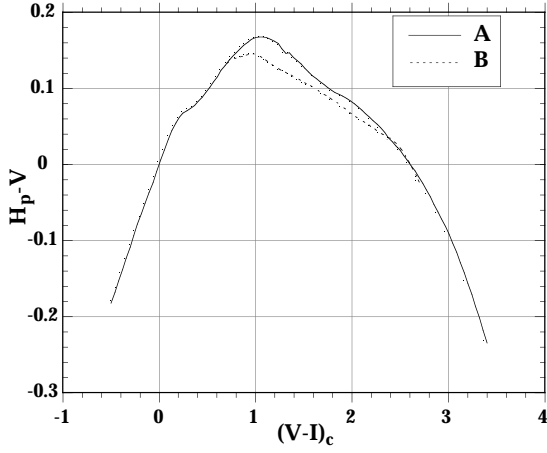


**Fig. 4.** Relation between  $(H_p - V_J)$  and the  $(V - I)_c$  colour index ( $H_p$  and  $V_J$  are resp. the Hipparcos global magnitude and the Johnson  $V$  magnitude). The solid curve (A) concerns the  $O$  to  $G5$  type stars of class  $V$  to  $II$ , and the red giants of types  $G5 III$  to  $M8 III$ . The dotted curve (B) holds for the  $G$ ,  $K$ , and  $M$  dwarfs with  $(V - I)_c > 0.7$ .

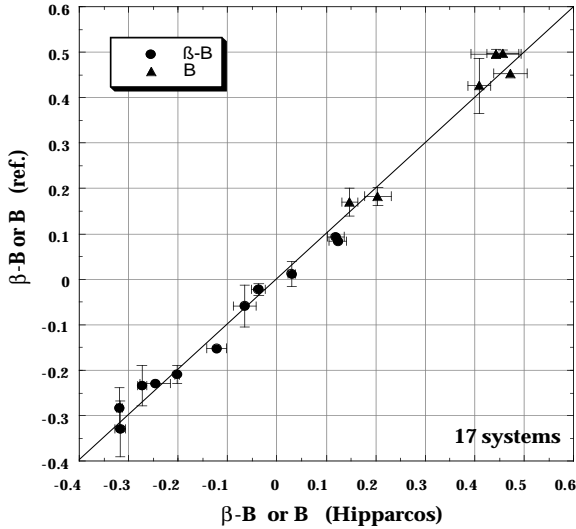


**Fig. 5.** Raw results of the processing: Comparison with ground-based measurements for 17 systems. For 11 double stars of Type II the difference  $\beta - B$  is plotted, while for 6 stars of type I the plotted value is the mass ratio  $B$  alone (upper part of the diagram). When available, the error bars are represented.

1. The Johnson's  $V - I$  index is first deduced from the spectral type by means of the data compiled in Zombeck, 1990.
2. This index is then converted into the Cousin's system as,

$$\begin{aligned} (V - I)_c &= 0.713 (V - I)_J & \text{if } (V - I)_J < 0 \\ (V - I)_c &= 0.778 (V - I)_J & \text{if } 0 \leq (V - I)_J \leq 2 \\ (V - I)_c &= 0.835 (V - I)_J - 0.13 & \text{if } 2 < (V - I)_J < 3.5 \end{aligned}$$

3. From  $(V - I)_c$  we get the quantity  $H_p - V_J$ , the difference between the Hipparcos magnitude and the Johnson  $V$  magnitude, by using the well calibrated relations presented in

**Table 6.** Spectral types and Johnson-Morgan's colour indices of the components of 18 double stars. The last column indicates the type of transformation to be made in order to get the Cousin's  $(V - I)$  index (see Fig. 4).

HIP	ST <sub>1</sub>	ST <sub>2</sub>	$(V - I)_1$	$(V - I)_2$	Conv.
171	G3 V	K6 V	0.87	1.77	A B
2762	F6 V	G1 V	0.68	0.83	A A
7580	F7 V	G0 V	0.72	0.81	A A
12390	F5 V	F5 V	0.64	0.64	A A
14328	B9 V	G8 III	-0.06	1.18	A A
14576	B8 V	F1 V	-0.12	0.51	A A
24608	G1 III	G8 III	1.11	1.18	A A
44248	F3 V	G5 V	0.58	0.89	A A
82817	M4.5 V	M4.5 V	3.33	3.33	B B
84140	M3 V	M4 V	2.94	3.19	B B
85141	G0 III	G0 III	1.09	1.09	A A
87895	G0-2 V	K2-5 V	0.83	1.42	A B
89937	F7 V	K0 V	0.72	1.06	A B
96683	K0 III	K0 III	1.30	1.30	A A
98416	F8 V	F8 V	0.76	0.76	A A
104858	F7 V	F7 V	0.72	0.72	A A
112158	G2 II-III	G8 II	1.14	1.20	A A
116849	F5 V	F5 V	0.64	0.64	A A

Fig. 4, which depend on the spectral type and class of the components.

4. Then, the Hipparcos magnitude difference  $\Delta m_H$  is deduced from the Johnson's by the expression:

$$\Delta m_H = \Delta m_V - (H_p - V_J)_1 + (H_p - V_J)_2$$

where  $(H_p - V_J)_1$  and  $(H_p - V_J)_2$  are related respectively to the primary and the secondary component.

When the spectral types of the two components are identical, the correction is equal to zero. For example, the correction for the well known system Algol  $AB - C$  reaches +0.11 mag.

### 5.3. Results and comments

The results are presented in Tables 7-8 respectively for 7 stars with solution of the first Type (direct determination of the mass ratio) and 36 stars of Type II. Even if the method 'A' is the most appropriate for the stars of Type I, the method 'B' has also been used for such systems for the sake of comparison. In all the cases, the individual masses obtained by either way are compatible. On the other hand, the method 'B' is the only one used for stars of Type II and then not mentioned in the table. When method 'A' is used, the magnitude difference is directly derived from the processing and thus does not need to be transformed into the Hipparcos system (there is a 'no' in the third column of Table 7). In all other cases,  $\Delta m$  comes from ground-based measurements (see references in Table 9) and a correction was applied whenever possible. The standard deviation on  $\Delta m$  has been taken equal to 0.15 mag whenever

it was unknown; the resulting errors on the masses  $M_1$  and  $M_2$  must then be regarded with caution. The ground-based  $\Delta m$  are of various origins: most of them come from the compilation files of the Observatory of the Côte d'Azur, some other from Worley, but whenever it was possible, we have chosen the most recently published result (see references in Table 9).

#### 5.4. Comparisons

An extensive bibliographical search has allowed to compare our results with ground-based measurements for 17 systems out of the 46 considered. For six stars of Type I on a total of eight, the mass ratios  $B$  have been directly compared, and for eleven stars of Type II for a total of thirty eight, the comparison refers to  $\beta - B$ . Results are shown in Fig. 5. It must be noted that the vertical error bars are not systematically present, as the standard deviations are not always available in the literature (the lack of error bar does not mean that the accuracy is outstanding!). In the same way, the Hipparcos and ground-based stellar masses have been compared for the same 17 systems. Results for each type are shown in Fig. 6.

Concerning the ratios, the general agreement between the two samples is excellent. For ten cases out of seventeen, the Hipparcos solution is more accurate than the ground-based one, or at worst simply identical. For five other cases it was not possible to conclude because of the absence of the standard deviation in the published data. When considering the masses of the components, the comparison reveals some disagreements related to the parallaxes. For such cases the error bars found in the literature are not of great help, as the uncertainties of the parallaxes are generally underestimated (especially for dynamical parallaxes).

The good agreement seen in the two samples seriously strengthens the confidence in the 29 other results, for which no ground-based estimate of mass ratio has been found. Moreover, one must keep in mind the principles of the method used here, which is mainly dependent on the quality of the orbital elements and, for Type II binaries, on the quality of the magnitude difference used to derive the individual masses.

The values presented in Table 9 are those used in this study to check the validity of our results. These are also the so called 'reference values' used as input of the algorithm to speed up the convergence of the process (see Sect. 3.2).

## 6. Comments on individual systems

### 6.1. Remarkable pairs

- *HIP 171 (85 Peg)*: the orbit of this visual and spectroscopic binary is very well known (flagged 'definitive' by Worley), even if its determination is not recent. The large semi-major axis (see Table. 2) is a very favourable instance for a direct determination of the mass ratio  $B$  based on the Hipparcos data. One of the peculiarities of this 'anomalous' system is that the mass of the secondary appears often larger than that of the primary, while the primary is much brighter ( $\Delta m > 3$  mag). This is why the companion 85 peg B is suspected to be an unresolved binary star (Heintz, 1993). At least six distinct determinations

of the individual masses of 85 Peg have been made between 1949 and 1992 (Fernandes, 1996), half of them giving the secondary more massive than the primary, but not significantly (according to the error bars). Feierman, 1971, has shown that for close pairs with  $\Delta m > 1.5$ , the  $\beta$  ratio was overestimated, which implies an overestimation of the mass ratio  $B$ , and thus of  $M_2$ , but his study is restricted to measurements made on photographic plates. There is no special reason to suspect such an effect with the present material. Moreover, the masses derived from the present study do not really allow to conclude: they do not significantly differ from one another ( $N = 1$  means that the standard errors of the masses are slightly underestimated, see Sect. 5.1).

- *HIP 2762 (13 Cet)*: this double-lined binary belongs to a set of 23 short period nearby G stars for which Duquennoy et al., 1991, have monitored the radial velocities. Mazej et al., 1992, have used these results to determine the mass ratio distribution. The large standard errors of the masses are probably realistic and follow from the relative smallness of the parallax: the parallax derived by Söderhjelm S., 1997, is larger than ours by only one mas and the semi-major axis smaller by six mas and this leads to a total mass 0.4 solar mass below the value derived here.

- *HIP 7580 (Kui 7)*: the old orbital solution given by Baize, 1985, and Heintz, 1988, yielded, with a distance of 42 pc, too small masses for a pair of late F/early G dwarfs (0.3 and 0.6  $M_\odot$  respectively). The new orbital elements taken from Hartkopf et al., 1996, result, with the old distance estimate, in a much reasonable value of 2.8  $M_\odot$  for the total mass. With the Hipparcos parallax, we obtain an intermediate value ( $\approx 2.1 M_\odot$ ), and a secondary component slightly more massive than the primary.

- *HIP 12390 ( $\epsilon$  Cet)*: A well known spectroscopic double-lined binary. The orbit is based uniquely on speckle data, which covers more than 4 revolutions. The new parallax estimate given by Hipparcos yields a total mass appreciably larger than before, while the mass ratio is slightly smaller (see Table 9).

- *HIP 14328 ( $\gamma$  Per)*: As  $\phi$  Cygni (HIP 96683), this spectroscopic binary contains highly evolved stars. The orbit is one of the most inclined ( $i \approx 90.5$  degrees) of this set. It is almost the more massive object of our study (after HIP 43671 = Fin 316). The masses and the parallax are in excellent agreement with the previous estimates (McAlister et al., 1982). The remark made for  $\gamma$  Per also holds true in the present case: the small value of the parallax results in a high relative error, and affects the quality of the sum of the masses.

- *HIP 19719 (46 Tau)*: Single lined spectroscopic and speckle binary. Thanks to speckle interferometry (Hartkopf et al., 1996), the orbit of this close binary is now very well known. Although the components are nearly equally bright, one of the stars seems clearly more massive than the other (the 'primary/secondary' status remains uncertain inside this object). At the moment, no

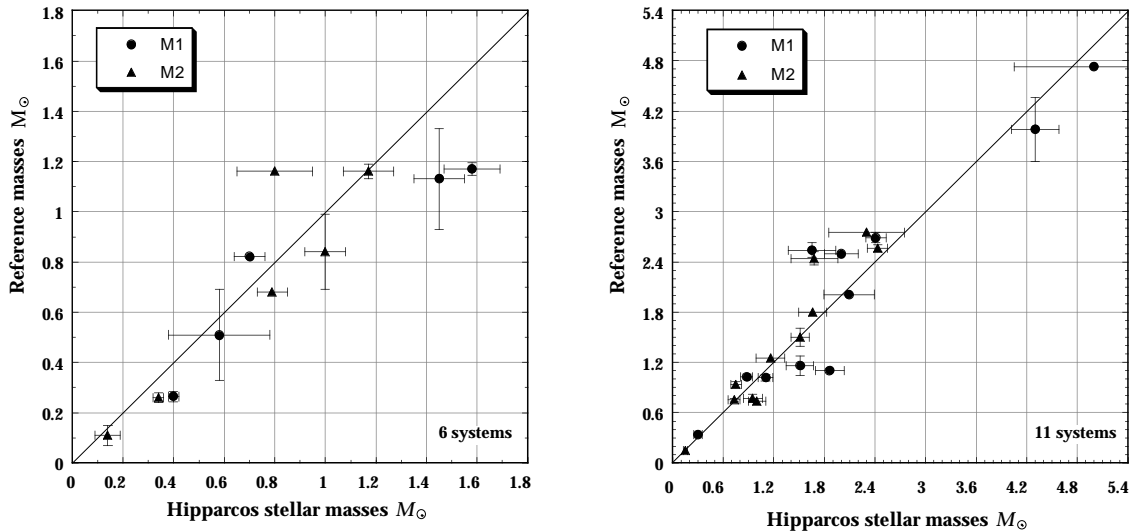


**Fig. 6a and b.** Stellar masses: Comparison with ground-based measurements for 17 systems. **a** 6 double stars of Type I; **b** 11 stars of type II (see text). When available, the error bars are represented.

comparison can be made because of the lack of other mass determination.

- **HIP 24608 (Capella)**: Famous double-lined spectroscopic binary, the brightest object of our sample ( $H_p = 0.24$ ). The masses derived here are slightly smaller than the commonly adopted values (Hummel et al., 1994a), due to the Hipparcos new estimate of the parallax. The extremely short period and the exceptional brightness of this pair could have resulted in better estimates than those presented in this paper had the orbit been larger.
- **HIP 44248 (10 Uma, Kui 37)**: As for 85 Peg (HIP 171), its large  $a$  and small  $P$  favour the direct estimate of the fractional mass  $B$ . The proposed solution is highly reliable.
- **HIP 45170 (81 Cnc, Fin 347 Aa)**: Visual, interferometric and spectroscopic solar-type binary, one of the shortest-period visual pairs (2.7 years, perfectly adapted to the Hipparcos time span). We have used the extremely precise orbit of Mason et al., 1996, yielding parallax and mass estimates in excellent agreement with his own determination. The present work tends to confirm the 'over-massive' status of this pair of G8-V stars.
- **HIP 75695 ( $\beta$  CrB)**: Cool Ap astrometric and spectroscopic binary star, and a famous magnetic variable. The new parallax estimate, four times more accurate than the previous one (Kamper et al., 1990), leads to a reduction of the error of the total mass by a factor six. Accurate estimates (10%) of the individual masses are proposed for the first time.
- **HIP 80346 (Gliese 623)**: Low mass short-period spectroscopic binary, one of the nearest pairs of our sample. The mass of the secondary component is expected to be near the substellar limit (Marcy et al., 1989). The authors mentioned a serious discrepancy between the dynamical mass estimates (0.51 and 0.11  $M_\odot$ ) and those deduced photometrically (0.34 and 0.084  $M_\odot$ ), a priori justified by a large underestimate of the parallax (134 mas).

With the new parallax estimate derived from the Hipparcos data ( $\pi \approx 125$  mas), this assumption is no longer valid. If the published orbital elements are correct (Henry et al., 1993), the real masses could be even slightly larger than the dynamical estimates. Nevertheless, the discussion is not completely settled, as the errors of the masses are still quite large (essentially due to the bad quality of the semi-major axis value).

- **HIP 84140 (Kui 79)**: This pair of dM3 red dwarfs is the nearest star of our sample ( $D \approx 6.5$  pc). Despite a good configuration for direct determination of the fractional mass (small period, large separation), Method B yields better estimates of the masses than those derived from Method A. In term of quality, these estimates are the best among the Type I stars (see Table 7). Masses of  $0.26 \pm 0.02 M_\odot$  for each component are proposed by Henry et al., 1993, assuming a semi-major axis  $a=0''.71$  and a parallax of nearly 160 mas. The new revised values,  $\pi = 152.2$  mas (this study) and  $a=0''.76$  (Hartkopf et al., 1996), yield larger masses: 0.40 and 0.34  $M_\odot$  with the same quality ( $0.02 M_\odot$ ).
- **HIP 86032 ( $\alpha$  Oph)**: Classical astrometric binary with a large magnitude difference. One of the most recently published photocentric orbits is that of Augensen et al., 1992, which is of no use in the frame of the present work. Augensen et al. provides also an estimate of the masses:  $M_1 = 2.0 M_\odot$  and  $M_2 = 0.5 M_\odot$ , which differ strongly from the estimates of Kamper et al., 1989: respectively 4.9 and 1.2  $M_\odot$ . The present solution (4.0 and 0.7  $M_\odot$ ) tends to confirm the previous one, with the reserve that the precisions are not very good.
- **HIP 89937 ( $\chi$  Dra)**: Nearby speckle and double-lined spectroscopic binary with solar-type primary component. This object is one of the few systems older than the Sun (about 8 billion years) whose parameters have been accurately determined, providing a benchmark for evolutionary theory. The masses pre-

**Table 7.** Masses of seven systems with solutions of first kind.

HIP	Method <sup>1</sup>	Corr. <sup>2</sup>	$\pi$ mas	$\sigma_\pi$ mas	$\Delta m^3$	$\sigma^4$	$M$ $M_\odot$	$\sigma$ $M_\odot$	$M_1$ $M_\odot$	$\sigma$ $M_\odot$	$M_2$ $M_\odot$	$\sigma$ $M_\odot$	$N^5$
171	A	no	82.16	1.27	3.27	0.87	1.494	0.069	0.705	0.060	0.789	0.063	1
171	B	yes	82.16	1.27	3.20	0.15	1.494	0.069	0.701	0.063	0.793	0.065	1
2762	A	no	46.74	0.97	1.29	0.31	2.852	0.425	1.711	0.306	1.141	0.239	3
2762	B	yes	46.74	0.97	0.75	0.15	2.852	0.425	1.425	0.258	1.427	0.258	3
44248	A	no	61.61	1.13	1.97	0.22	2.445	0.135	1.445	0.098	1.000	0.079	3
44248	B	yes	61.61	1.13	2.08	0.15	2.445	0.135	1.473	0.102	0.972	0.081	3
80346	A	no	125.56	1.63	3.89	0.50	0.723	0.252	0.575	0.202	0.147	0.055	3
80346	B	no	125.56	1.63	5.50	0.79	0.723	0.252	0.590	0.206	0.132	0.047	3
84140	A	no	152.2	1.82	0.45	0.08	0.748	0.027	0.417	0.040	0.331	0.039	3
84140	B	yes	152.2	1.82	0.38	0.15	0.748	0.027	0.404	0.020	0.344	0.018	3
86032	A	no	69.09	1.01	5.23	2.33	4.710	0.760	4.018	0.653	0.692	0.135	3
86032	B	no	69.09	1.01	3.50	0.15	4.710	0.760	3.875	0.631	0.835	0.157	3
104858	A	no	54.69	1.00	0.02	0.09	2.759	0.151	1.498	0.121	1.261	0.112	1
104858	B	yes	54.69	1.00	0.29	0.15	2.759	0.151	1.670	0.108	1.089	0.083	1

<sup>1</sup> Method A: the ratios  $\beta$  and  $B$  are solutions of our processing.  $\Delta m$  is directly deduced from  $\beta$ . Method B: the mass ratio  $B$  is deduced from the solution ( $\beta - B$ ) and a  $\Delta m$  estimate taken from the literature.

<sup>2</sup> Correction: when Method B is used, 'yes' indicates that the  $\Delta m$  estimate has been converted into the Hipparcos photometric system, via the spectral types of the components (see Sect. 5.2).

<sup>3</sup> It is the Hipparcos estimate if Method A is used, a ground-based one otherwise.

<sup>4</sup> When unknown,  $\sigma$  is taken equal to 0.15.

<sup>5</sup> Number of available terms for the computation of the standard deviation of the total mass  $M$ .  $N = 3$  if  $\sigma_a$ ,  $\sigma_\pi$  and  $\sigma_P$  are known.  $N = 2$  if  $\sigma_P$  is unknown.  $N = 1$  if both  $\sigma_a$  and  $\sigma_P$  are ignored. In the latter case,  $\sigma(M)$  is underestimated.

sented in this study are in satisfactory agreement (especially for the primary) with the old estimates of McAlister (1980):  $0.88 \pm 0.09$  and  $0.67 \pm 0.05 M_\odot$ , but not with the results taken from the more recent work of Tomkin et al., 1987 ( $1.03 \pm 0.03$  and  $0.75 \pm 0.02 M_\odot$ ), whose main purpose was precisely to update the mass estimates of McAlister, qualified as "surprisingly low for a system with an F7 V primary". This discrepancy holds however only for the mass of the primary.

- **HIP 96683** ( $\phi$  Cyg): Famous double-lined spectroscopic binary, formed by two 'normal' giants with comparable magnitudes and spectral types. The very small orbit ( $a'' \approx 23$  mas) is based on observations carried out with the Mark III Interferometer. The mass ratio proposed here is fully reliable, but the total mass is very sensitive to the value adopted for the parallax. For example, adopting  $\pi = 13.0$  mas instead of  $\pi = 14.1$  mas yields a total mass of  $4.3 M_\odot$  instead of  $3.35 M_\odot$ . The individual masses are indeed probably larger than those announced here, according to the numerous works on that system. The knowledge of the orbit size must be improved.

- **HIP 104858** ( $\delta$  Equ): Spectroscopic binary with solar type primary. As for HIP 171, the errors of the orbital elements are ignored, so that the mass estimates of Table 7 should be affected by a larger error. Compared to previous determinations, the mass of the primary seems somewhat overestimated. A more reliable orbit is awaited for confirmation.

- **HIP 112158** ( $\eta$  Peg): Spectroscopic and interferometric binary containing a G2II-III giant, one of the smallest orbit in our sample. Although no information could be found on the masses, the mass estimates presented in Table 8 are consistent with the position of the components in the HR diagram.

## 6.2. The case of Algol

Because of its photometric peculiarities, the eclipsing system Algol AB-C (HIP 14576) deserves a special treatment. Due to its small separation, the contact eclipsing binary A-B is equivalent, for Hipparcos, to a variable single star. Associated to the C dwarf, this triple system thus shows up as an astrometric binary with a variable component. Between March 1990 and February 1993, the Algol system has been observed 81 times on the modulating grid of the Hipparcos instrument (each observation is a 19 s transit across the whole grid), corresponding to 24 different epochs (two consecutive epochs being separated by about six weeks). The resulting photometric curve of Fig. 7 has been built from this material and the information on the phase (Söderhjelm S., 1980),

$$\phi_{AB} = (t - 2445641.514) / 2.86734 \quad (8)$$

where  $t$  is the observation time in JD. The curve reveals five 'atypical' observations located during the eclipse, with discrepant magnitudes from the rest of the distribution. The lowest magnitude transit is exactly located during the deepest eclipse

**Table 8.** Astrometric binaries processing. Masses for 36 systems with solutions of second kind.

HIP	Correction	$\pi$ mas	$\sigma_\pi$ mas	$\Delta m$	$\sigma$	$M$ $M_\odot$	$\sigma$ $M_\odot$	$M_1$ $M_\odot$	$\sigma$ $M_\odot$	$M_2$ $M_\odot$	$\sigma$ $M_\odot$	$N$
2237	no	30.24	0.98	0.060	0.150	2.800	0.272	1.492	0.153	1.308	0.136	1
7580	yes	26.22	1.08	0.411	0.150	2.112	0.282	0.890	0.139	1.222	0.178	3
12390	yes	26.22	1.08	0.060	0.150	2.876	0.258	1.886	0.171	0.990	0.092	3
14328	yes	13.67	0.85	1.567	0.150	7.332	1.368	5.036	0.951	2.295	0.453	1
14576	yes	34.77	0.74	3.030	0.150	5.812	0.373	4.302	0.281	1.510	0.110	3
19508	no	16.00	1.05	0.100	0.150	1.861	0.366	1.036	0.209	0.824	0.168	1
19719	no	26.11	0.96	0.150	0.150	2.712	0.303	1.086	0.133	1.626	0.190	3
22196	no	13.38	1.12	0.010	0.150	5.928	1.489	3.061	0.775	2.867	0.727	1
24608	yes	77.13	0.94	0.154	0.050	4.839	0.177	2.412	0.124	2.427	0.125	3
29850	no	12.90	1.06	0.150	0.150	4.048	1.004	2.115	0.554	1.933	0.511	3
31509	no	23.92	0.63	0.400	0.150	2.230	0.176	1.006	0.160	1.224	0.169	1
38052	no	26.20	0.93	0.100	0.150	1.765	0.190	1.096	0.162	0.669	0.133	3
39261	no	10.56	0.79	0.050	0.150	3.271	0.801	0.502	0.301	2.769	0.732	3
43671	no	12.01	0.64	0.010	0.150	12.39	1.980	9.406	1.595	2.982	0.715	1
45170	no	48.24	1.02	0.400	0.150	1.908	0.153	1.072	0.087	0.836	0.068	3
54204	no	23.01	0.86	0.100	0.150	4.113	0.461	2.225	0.261	1.888	0.226	1
64838	no	12.92	0.95	0.010	0.150	2.869	0.684	1.616	0.422	1.253	0.345	3
75695	no	27.48	0.82	1.600	0.120	3.632	0.334	1.963	0.193	1.668	0.168	3
82817	yes	159.70	2.98	0.180	0.150	0.865	0.048	0.354	0.021	0.511	0.029	1
83838	no	18.22	0.72	0.130	0.150	3.496	0.415	2.041	0.246	1.455	0.178	3
85141	yes	15.00	1.21	0.010	0.150	4.454	1.148	1.511	0.470	2.943	0.802	3
87204	no	18.99	0.69	0.010	0.150	1.948	0.220	0.834	0.153	1.114	0.174	3
87655	no	15.66	0.81	0.200	0.150	2.175	0.361	1.653	0.289	0.522	0.126	3
87895	yes	35.04	0.88	2.822	0.300	2.455	0.253	1.509	0.167	0.946	0.115	3
89937	yes	123.93	0.47	2.023	0.390	1.617	0.044	0.884	0.072	0.733	0.071	3
91394	no	19.66	1.06	0.130	0.150	2.892	0.468	1.932	0.360	0.960	0.237	3
93574	no	17.20	0.61	0.010	0.150	3.539	0.377	1.594	0.176	1.945	0.212	1
94349	no	97.70	4.63	2.700	0.150	0.445	0.063	0.302	0.045	0.144	0.025	1
94739	no	62.76	1.96	0.010	0.150	0.895	0.084	0.556	0.079	0.339	0.067	1
96683	yes	14.13	0.58	0.300	0.200	3.346	0.445	1.648	0.277	1.697	0.283	3
98416	yes	39.20	1.53	0.010	0.150	2.247	0.266	1.758	0.306	0.489	0.232	3
105431	no	20.73	0.97	0.100	0.150	3.255	0.457	2.089	0.298	1.165	0.173	1
107354	no	28.63	0.92	0.400	0.150	4.173	0.412	1.799	0.188	2.374	0.243	3
108431	no	17.68	0.94	0.100	0.150	4.945	0.789	2.156	0.536	2.789	0.605	1
112158	yes	16.48	0.98	3.703	0.150	4.072	0.727	2.773	0.498	1.299	0.238	2
116849	yes	13.96	0.96	0.300	0.150	2.723	0.563	1.257	0.326	1.466	0.361	3

phase, which lasts about 20 minutes. In order to get a photometrically homogeneous set of observations, consistent with the input value of the magnitude difference outside the eclipses (see Table 9), these few observations have been excluded from the analysis. Owing to the precisions involved, it was not necessary to eliminate the few observations located at  $\phi_{AB} = 0.5$  (secondary minimum of the curve). The quantity  $\beta - B$  derived for Algol is one of the most precise determinations. The stability of the solution is excellent. It is not sensitive to the choice of the input values for  $\beta$  and  $B$ , and does not depend too much on the weighing of the observations. This result is in good agreement with the previous determination of Pan et al., 1993, which provides also a very reliable orbit.

## 7. Further works

This study has been essentially limited by the approximate knowledge of several parameters taken from various sources (the ground-based orbital elements in the present case). For more than two thirds of the 145 selected objects, an improvement of the orbits is highly desirable to improve the quality of the results. An interesting direction to be explored, consists of the direct use of the individual relative positions of the components (separation  $\rho$  and position angle  $\theta$  at precise dates) on the arc of orbit corresponding to the Hipparcos observation's epochs. By this way, the number of candidates should be largely increased, since the complete orbit is no longer needed to perform the processing: a polynomial fit in the interesting area should be sufficient to interpolate the separation  $\rho$  at a given date. Finally,

**Table 9.** Reference values of component masses and physical ratios.

HIP	$M_1$ $M_\odot$	$\sigma$ $M_\odot$	$M_2$ $M_\odot$	$\sigma$ $M_\odot$	$B$	$\sigma$	$\beta$	$\sigma^*$	references
171	0.82	—	0.68	—	0.453	—	0.050	0.009	Belikov95, Eggen56
12390	1.10	—	0.74	—	0.402	—	0.486	0.046	Belikov95, Mazeh92
14328	4.73	—	2.75	—	0.368	—	0.216	0.031	McAlister92
14576	3.98	0.38	1.50	0.11	0.274	0.024	0.064	0.008	Pan93
24608	2.69	0.06	2.56	0.04	0.488	0.007	0.466	0.011	Hummel94b
44248	1.13	0.20	0.84	0.15	0.426	0.061	0.132	0.021	Belikov95, Eggen56
45170	1.015	0.038	0.933	0.039	0.452	—	0.409	0.044	Mason96
75695	2.5	—	1.8	—	0.420	0.040	0.186	0.017	Hummel94a
80346	0.51	0.18	0.114	0.04	0.183	0.020	0.006	0.005	Belikov95, Henry93
84140	0.264	0.02	0.260	0.02	0.496	0.010	0.409	0.044	Henry93
86032	4.94	—	1.16	—	0.170	0.030	0.038	0.007	Kamper89
87895	1.16	0.12	0.77	0.05	0.399	0.059	0.070	0.018	McAlister95
89937	1.03	0.03	0.75	0.02	0.421	0.010	0.138	0.043	Tomkin87
94349	0.34	—	0.15	—	0.306	—	0.077	0.013	Harrington77
96683	2.54	0.09	2.44	0.08	0.490	0.012	0.431	0.045	Belikov95
104858	1.17	0.025	1.16	0.03	0.497	0.008	0.433	0.045	Armstrong92b
105431	2.01	—	1.25	—	0.383	—	0.477	0.046	West81

\* When unknown, the error on the magnitude difference is taken equal to 0.2, in order to estimate  $\beta$ .

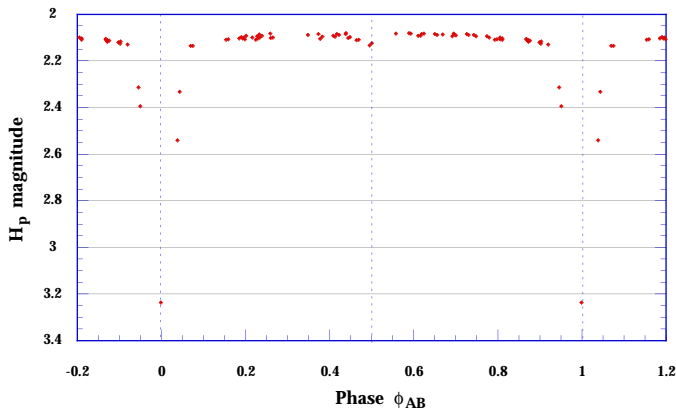


**Fig. 7.** Light curve of Algol AB-C (HIP 14576), derived from the Hipparcos observations. The deepest minimum ( $H_p = 3.237 \pm 0.003$ ) corresponds to the occultation of the bright B type component by the K0 IV red subgiant. The symmetrical situation ( $\phi = 0.5$ ) produces a minimum at  $H_p \approx 2.13$  mag.

the survey of short period systems undertaken for this study is not comprehensive, and a more extensive research is planned for the next coming months.

## 8. Conclusion

This work provides an additional example of the hidden resources embedded in the Hipparcos observations. While the idea of studying the astrometric binaries from the absolute positions of the photocentre was put forth at an early stage during the mission design, the fact that the fiducial point observed through the modulating grid was not the system photocentre came much

later after months of analysis of anomalous residuals of the astrometric processing. This opportunity has been fully exploited in this paper to determine for a handful systems the mass of each of the components and the individual brightness together with the parallax. For the remaining 37 close binaries with short periods, the introduction in the modelling of the orbital motion has allowed to derive a more accurate parallax than with the standard Hipparcos processing and to determine a function of the mass ratio and of the magnitude difference.

*Acknowledgements.* Useful discussions with M. Fréschlé during the preparation of this paper are gratefully acknowledged.

## References

- Armstrong J.T. et al., 1992a, *Astron. J.*, 104, No. 1, 241.
- Armstrong J.T. et al., 1992b, *Astron. J.*, 104, No. 6, 2217.
- Augensen H.J. et al., 1992, *Publ. Astron. Soc. Pac.*, 104, 314.
- Baize P., 1988, *A&A Suppl. Ser.*, 60, 333.
- Baize P., 1993, *A&A Suppl. Ser.*, 99, 205.
- Belikov A.N., 1995, *Bull. Inf. CDS* 47, 9.
- Churms J., 1965, thesis, Univ. Witwatersrand.
- Duquenooy, A., Mayor, M., Halbwachs, J.L., 1991, *A&A Suppl. Ser.*, 88, 281.
- Eggen O.J., 1956, *Astron. J.*, 61, No. 1242, 361.
- ESA 1997, *The Hipparcos and Tycho Catalogues*, SP-1200.
- Feierman, B.H., 1971, *Astron. J.*, 76, 73.
- Fernandes, J., 1996, Thesis.
- Finsen W.S., 1973, *Circ. Inf. No.* 60.
- Finsen W.S., 1977, *Circ. Inf. No.* 71.
- Hall R.G. et al., 1949, *Astron. J.*, 54, 102.
- Harrington R.S., 1977, *Publ. Astron. Soc. Pac.*, 89, 214.
- Hartkopf W.I. et al., 1989, *Astron. J.*, 98, No. 3, 1014.
- Hartkopf W.I. et al., 1996, *Astron. J.*, 111, No. 1, 370.

- Heintz W.D., 1984, *Astron. J.*, 89, No. 7, 1063.  
Heintz W.D., 1988, *A&A Suppl. Ser.*, 72, 543.  
Heintz, W.D., 1993, *Astron. J.*, 105, 1188.  
Henry T.J. et al., 1993, *Astron. J.*, 106, No. 2, 773.  
Hummel C.A. et al., 1992, *ESO Conference on High-Resolution Imaging by Interferometry II, Part II*, 697.  
Hummel C.A. et al., 1994a, *Astron. J.*, 107, No. 5, 1859.  
Hummel C.A. et al., 1994b, *Very High Angular Resolution Imaging*, IAU, 410.  
Kamper K.W. et al., 1989, *Astron. J.*, 98, No. 2, 686.  
Kamper K.W. et al., 1990, *Astron. J.*, 100, No. 1, 239.  
McAlister H.A. et al., 1982, *Astron. J.*, 87, No. 3, 563.  
McAlister H.A. et al., 1995, *Astron. J.*, 110, No. 1, 366.  
Marcy G.W. et al., 1989, *Astrophys. J.*, 341, 961.  
Martin, C., Mignard, F., Fröeschlé, M., 1997, *A&A Sup. Ser.*, 122, 571-580.  
Mason B.D. et al., 1996, *Astron. J.*, 112, No. 1, 276.  
Mazeh T. et al., 1992, *Astrophys. J.*, 401, 265.  
Mignard, F., Fröeschlé, M., Badioli, M. et al, 1992, *A&A*, 258, 165.  
Mignard, F., Söderhjelm, S., Bernstein, H. et al., 1996, *A&A*, 304, 94.  
Muller P. et al., 1954, *J. Observateurs*, 37, 64.  
Pan X. et al., 1993, *Astrophys. J.*, 413, 129.  
Söderhjelm S., 1980, *A&A*, 89, 100.  
Söderhjelm S., Lindegren L. & Perryman M., 1997, *Hipparcos Venice '97*, ESA SP-402, M. Perryman & P.L. Bernacca eds.  
Tomkin J. et al., 1987, *Astron. J.*, 93, No. 5, 1236.  
Van den Bos W.H., 1953, *Union Obs. Circ.*, 6, 216.  
Van den Bos W.H., 1956, *Union Obs. Circ.*, 6, 279.  
Van den Bos W.H., 1957, *Union Obs. Circ.*, 6, 290.  
Voute J., 1946, *Riverview Coll. Obs. Pub*, 2, 43.  
West F.R. et al., 1976, *Astrophys. J.*, 205, 194.  
West F.R. et al., 1981, *BAAS*, 13, 569.  
Worley C.E. & Heintz W.D., 1983, *The fourth catalog of orbits of visual binary stars*, *Publ. U.S. Naval Obs.* (2) 24, part VII.  
Zombeck M.V., 1990, *Handbook of Space Astronomy & Astrophysics*, Cambridge U.P.